

Cuprous oxide nanocubes functionalized with graphene quantum dots and its application for methylene blue degradation

Tran Thi Bich Quyen^{*a}, Pham Hai Dang^a, Ngo Nguyen Tra My^a, Duy Toan Pham^b, Doan Van Hong Thien^a, Luong Huynh Vu Thanh^a

a) Department of Chemical Engineering, College of Technology, Can Tho University, 3/2 Street, Ninh Kieu District, Can Tho 900000, Vietnam

b) Department of Chemistry, College of Natural Sciences, Can Tho University, 3/2 Street, Ninh Kieu District, Can Tho 900000, Vietnam

Received 14 November 2021; received in revised form 29 January 2022; accepted 18 February 2022

ABSTRACT

Cuprous oxide nanocubes (Cu₂O NCBs) were successfully functionalized with graphene quantum dots (GQDs) to form GQDs/Cu₂O NCBs composites material with highly plasmonic property and photocatalytic activity. Herein, GQDs were synthesized by a hydrothermal method at 190°C for 8 h using natural sources of wheat flour and ascorbic acid as precursors and reducing agents, respectively. Cu₂O NCBs were prepared via a simple chemical reduction method at room temperature. GQDs/Cu₂O NCBs composites were fabricated by the simple mixing of the two corresponding component dispersions. Characterized by ultraviolet-visible spectroscopy (UV-Vis), Fourier transform infrared spectroscopy (FTIR), X-ray diffractometry (XRD), transmission electron microscopy (TEM), and energy-dispersive X-ray spectroscopy (EDX), the GQDs/Cu₂O NCBs structures were confirmed. The composites possessed cubic shape of Cu₂O and spherical shape of GQDs with average particle sizes respectively being ~70-80 nm, and ~3-8 nm; and an elemental composition of C (41.53%), O (47.03%), N (0.24%), and Cu (11.20%). Moreover, experiments on the methylene blue (MB) degradation demonstrated that the GQDs/Cu₂O NCBs composites significantly degraded >98% of the total dye amount within 30 min. In summary, the novel composites possessed potential high catalytic activity and could be utilized as photocatalysts in the treatment of organic pollutants and biological waste such as dyes, antibiotics, and pesticides.

Keywords: Graphene quantum dots (GQDs); Cuprous oxide nanocubes (Cu₂O NCBs); Photocatalytic activity; Wheat flour; Methylene blue (MB)

1. Introduction

The increase of organic pollutants in the aquatic environment has been recorded worldwide due to the increase in world population and the continuous development of industries and agriculture [1]. Wastewater from a number of industries such as pharmaceuticals, textiles, and also from dye that often contains toxic pollutants with low biodegradability. Although many chemical treatment methods have been applied, oxidants used in water treatment processes have difficulty in decomposing and mineralizing pollutants with complex structures.

All these methods have some disadvantages such as: incomplete removal, high energy requirements, high cost (activated carbon) and generation of other wastes that require further treatment [2]. Recently, studies using strong oxidants such as OH free radicals are emerging as an effective method to degrade toxic water pollutants. Among them, the photocatalysis method is noticed as a green, eco-friendly, low-cost method with high degradation efficiency [3, 4].

Photocatalysis is a promising method for the degradation of inorganic and organic pollutants in the environment, especially in air and water. In this photocatalysis process, irradiation of semiconductors by UV-Vis photons with sufficient energy causes the generation of electron-hole pairs (e⁻/h⁺). These e⁻/h⁺

^{*}Corresponding author:

E-mail address: ttbquyen@ctu.edu.vn (T. Quyen)

pairs then immediately react with dissolved oxygen and water/hydroxyl to produce superoxide and hydroxyl radicals, respectively. These powerful oxidants will directly interact with the organic molecules in the pollutants, breaking them down into smaller compounds and eventually into water and carbon dioxide. Many studies have shown that combining semiconductors with suitable support will limit the instinctive defect that limits the catalytic activity of semiconductors, which is the rapid recombination of electron and hole pairs [5, 6].

Recently, metal oxide-based photocatalysts have gained increasing consideration as important functional materials in numerous applications due to their unique and adjustable properties [7-9]. Amongst various metal oxide, cuprous oxide (Cu_2O), a p-type semiconductor with a 2.17 eV direct band gap. Due to its band structure, Cu_2O can absorb visible light, which is the main ground-dispersed solar radiation [10]. Therefore, in principle, Cu_2O is a promising catalyst. Cu_2O nanocrystals have been extensively studied for water separation and decomposition of organic pollutants under visible light irradiation [11-14] and also it has adopted a wide application in photoelectrolytic cells, etc [15, 16]. However, the application of Cu_2O in photocatalysis is limited due to its low quantum efficiency, photo corrosion drawbacks, and the rapid recombination of the photogenerated charge carriers [14]. Interestingly, the Cu_2O catalytic capacity is heavily affected by the structure-related band gap energy and the surface modification from other elements/molecules on the basis of diminishing the e^-/h^+ recombination. For instance, the $\text{Cu}_2\text{O}-\text{Cu}-\text{Cu}_2\text{O}$ nanocomposites significantly increased the catalytic action in 4-nitrophenol reduction compared to the Cu_2O alone [13]. $\text{Cu}_2\text{O}-\text{TiO}_2$ nanotubes and $\text{Cu}_2\text{O}-\text{ZnO}$ nanowires could effectively degrade the rhodamine B dye better than the Cu_2O [17, 18]. To this end, a potential approach is to functionalize the Cu_2O with materials that can alter its surface properties to enhance its catalytic activity. A possible material, in this case, was graphene quantum dots (GQDs).

Carbon-based materials such as graphite carbon nitride (g-C₃N₄) have unique optical, electrical, and physicochemical properties and have been extensively explored for energy generation and environmental remediation applications [19]. However, intrinsic limitations of g-C₃N₄, such as poor mass diffusion, and rapid recombination of photoelectric charges limit its application in catalytic reaction [20]. Graphene, a nanocarbon material, has been widely investigated due to its excellent properties namely high surface area, large carrier mobility, good

fluorescence/thermal/chemical stability, mechanical flexibility, and biocompatibility [21, 22]. Because of these fascinating physical properties, graphene has been explored intensively for photocatalysis. Amongst many graphene structures (i.e., nanosheets, nanoribbons), GQDs are commonly employed in numerous applications such as biomedicine, optoelectronics, sensing, and catalysis, due to their high quantum confinement and boundary effects, tuneable luminescence properties, low toxicity, hydrophilic nature, excellent photo-stability, high specific surface area and abundance of raw materials [23-25]. GQDs have an sp^2 hybridized two-dimensional (2D) honeycomb lattice structure with excellent electron transfer and acceptor properties along with stable photoluminescence. Therefore, the integration of GQDs with photoactive semiconductors is prompting research into new materials suitable for photocatalytic applications. Kumar et al [25] synthesized GQDs/ZnO heterojunction in nanostructure with large specific surface area to degrade methylene blue dye (MB) and colorless pollutant (carbendazim fungicide) with high photocatalytic efficiency. Generally, GQDs are synthesized through cutting carbonic precursors, such as graphene, graphene oxide and carbon fibers, into smaller pieces by chemical oxidation, hydrothermal, or solvothermal treatment under harsh conditions with the use of sulfuric acid, nitric acid or other strong oxidizers [26]. However, none of these methods are regarded as green and they possess many unavoidable drawbacks of (1) potential safety risks and environmental pollution, (2) high cost and complex fabrication process, and (3) complicated post-processing procedure [27]. Thus, eco-friendly alternative methods with green precursors such as wheat flour are better approaches [28, 29].

In this work, the GQDs/ Cu_2O NCBs nanocomposites were fabricated and their photocatalytic activity on methylene blue degradation was evaluated. We hypothesized that the novel, previously unreported incorporation of GQDs on the surface of Cu_2O NCBs incorporation of GQDs on the surface of Cu_2O NCBs could prevent the recombination of electron and hole pairs, thus, increasing the particle surface area and enhancing the photocatalytic activity. GQDs were synthesized by hydrothermal method at 190 °C for 8 h using natural sources from wheat flour and ascorbic acid as precursors and reducing agents. Cu_2O NCBs were prepared via a simple chemical reduction method at room temperature. The functionalization process was conducted by simple mixing of the two component dispersions at room temperature for 60 min. The products were characterized in terms of ultraviolet-visible spectroscopy (UV-Vis), Fourier transform

infrared spectroscopy (FTIR), X-ray diffractometry (XRD), transmission electron microscopy (TEM), and energy-dispersive X-ray spectroscopy (EDX) analyses. Finally, the composite photocatalytic ability, and the effects of composite amounts and absorption time, on the methylene blue degradation were investigated using UV-Vis spectroscopy, results show the catalytic potential of GQDs/Cu₂O NCBs when removing >98% MB in 20 min in a simple reaction.

2. Experimental

2.1 Materials

Wheat flour was purchased from Vincom Xuan Khanh supermarket (Ninh Kieu, Can Tho, Vietnam). Copper sulfate pentahydrate (CuSO₄.5H₂O), hydrazine hydrate (N₂H₄.2H₂O), D-glucose (C₆H₁₂O₆), ascorbic acid (C₆H₈O₆), sodium hydroxide (NaOH), hydrogen peroxide (H₂O₂), polyvinylpyrrolidone (C₆H₉NO)_n, and methylene blue (C₁₆H₁₈ClN₃S.3H₂O) were imported from Sigma-Aldrich. All chemicals and solvents used were of reagent grade. All solutions were prepared with deionized water (DI H₂O) from a MilliQ system.

2.2 Preparation of GQDs

To manufacture the GQDs, a starch solution was first prepared by dissolving 0.3 gram of wheat flour in 12 mL distilled water and heated at 60°C for 30 min. Then, 2 mL of ascorbic acid (1 M) was slowly added into the starch solution, followed by stirring for 5 min. Next, the mixture was transferred into a 15-mL autoclave reactor and heated at 190°C for 8 h to complete the reaction. Finally, the mixture was centrifuged and washed with DI H₂O several times to remove the precipitates, resulting in the GQDs dispersion.

2.3 Preparation of Cu₂O NCBs

Cuprous oxide nanocubes (Cu₂O NCBs) were prepared following a protocol reported in a previous study with some modification [30]. Briefly, 0.0703 gram CuSO₄.5H₂O and 0.361 gram D-glucose were dissolved in 100 mL double distilled water and stirred for 15 min. Then, 100 microliters (μL) of NaOH (10 M) was added dropwise into the solution to yield a blue colored solution of Cu(OH)₂. After 15 min of stirring, 200 μL of 2M N₂H₄ solution was dropped into this solution, making the solution color gradually change from blue to brick red. The solution was stirred until the Cu(OH)₂ precipitates were completely reduced by the hydrazine hydrate. Finally, the obtained products, brick red solid particles, were centrifuged for 20 min at 4000 rpm,

washed with DI H₂O to neutrality, and dispersed in 10 mL of DI H₂O for further experiments.

2.4 Preparation of GQDs/Cu₂O NCBs

To synthesize the GQDs/Cu₂O NCBs composites, PVP solution (5 mg.mL⁻¹ in DI H₂O) was added to 5 mL of the Cu₂O NCBs dispersion and stirred for 30 min at room temperature. Then, GQDs dispersions, at different amounts of 0.5, 1.0, 1.5, and 2.0 mL, were slowly added and stirred continuously for 30 min. The GQDs/Cu₂O NCBs were formed spontaneously.

2.5 Characterizations of GQDs/Cu₂O NCBs

To characterize the GQDs/Cu₂O NCBs composites, as well as their GQDs counterparts for comparison purposes, UV-Vis spectroscopy was observed by recording the absorbance spectra between 200 and 900 nm on the UV-vis spectrophotometer (Thermo Scientific Evolution 60S UV-Vis spectrophotometer, USA). X-ray diffraction (XRD) was performed on a D8-Advance machine (Bruker, Germany) in the 2θ range of 10°-80°. The Fourier transform infrared (FT-IR) spectra were obtained by Perkin Elmer Frontier MIR/NIR (Perkin Elmer, USA) in the range of 4000-400 cm⁻¹. Transmission electron microscopy (TEM) characterization was performed on a Jem1010 device (Joel Company, Japan). Chemical properties and constituent components were analysed via Energy-dispersive X-ray spectroscopy (EDX H-7593, Horiba, England).

2.6 Photocatalytic ability investigations of GQDs/Cu₂O NCBs composites on MB degradation

The photocatalytic ability of GQDs/Cu₂O NCBs composites on MB degradation was determined at different composite amounts and reaction times. Firstly, the effects of GQDs/Cu₂O NCBs composites amount on their ability were investigated. For this reason, 10 mL of MB solution (10 mg.L⁻¹) was treated with different amounts of GQDs/Cu₂O NCBs composites (i.e., 0, 250, 500, 750, and 1000 μL) and 500 μL H₂O₂ for 30 min. A corresponding amount of distilled water was added to the mixtures to obtain the same solution volumes.

The suitable amount of GQDs/Cu₂O NCBs was further investigated in terms of the reaction time. To this end, 10 mL of MB solution (10 mg.mL⁻¹ in DI H₂O) was treated with the optimal amount of GQDs/Cu₂O NCBs composites and 750 μL H₂O₂ for 10, 20, 30, and 40 min, respectively. UV-Vis spectroscopy was utilized to investigate the MB degradation. The degree of degradation was calculated based on the MB original

peaks and the corresponding peaks of the GQDs/Cu₂O NCBs composites/MB spectra. All experiments were adjusted and maintained at pH = 7.

2.7 Statistical analysis

All experiments and analyses were conducted in triplicate to confirm the outcomes. The results were expressed as average data from the three measurements.

3. Results and Discussion

3.1 Preparation of GQDs/Cu₂O NCBs

This work demonstrated novel composites fabricated from GQDs and Cu₂O NCBs for its photocatalytic ability on MB degradation. The GQDs were made from wheat flour and their properties were similar to previous reports [31]. On the other hand, the Cu₂O NCBs formulating process was modified from other study [30] with better outcomes. The reaction time was significantly reduced from 30 min to 15 min, and the obtained NCBs had smaller particle sizes of 70-80 nm compared to 100-150 nm. Thus, our process might improve the Cu₂O NCBs properties by adjusting the reactant ratios and formulation parameters.

Since the incorporation of GQDs on the surface of Cu₂O NCBs could prevent the recombination of electron and hole pairs on the material surface structure, this contributes to an increase in the particle surface area, thereby enhancing the photocatalytic activity of Cu₂O NCBs. Furthermore, the epoxy groups (C-O-C) located on the GQDs contribute to the natural linkages between them and the NCBs, making it easier to fabricate the composites materials [32]. For this reason, the GQDs/Cu₂O NCBs were successfully formulated, and their properties were dependent on the amount of GQDs. **Fig. 1** shows the UV-Vis spectra of GQDs/Cu₂O NCBs composites at different added GQDs amounts. The absorption peak at 300 nm corresponds to the Cu⁺ ions, whereas the peak at 318 nm is the Cu²⁺ signal. As the volumes of GQDs solutions increased to 1.5 and 2 mL, the Cu²⁺ peak appeared due to the low pH of the GQDs solutions, which caused a redox reaction and produced Cu²⁺ ions. Therefore, the suitable GQDs volume was 1 mL to preserve the Cu₂O NCBs properties and fabricate the GQDs/Cu₂O NCBs at the same time.

3.2. Characterizations of GQDs/Cu₂O NCBs

The novel GQDs/Cu₂O NCBs were thoroughly characterized in terms of FTIR, XRD, TEM, and EDX methods. In the GQDs FTIR spectrum (**Fig. 2**), the wide absorption band at 3376 cm⁻¹ corresponds to the stretching vibration of O-H. A small fluctuation at 2927

cm⁻¹ is the characteristic peak of the C-H functional group [33]. The weak peak at 1198 cm⁻¹ represents the C-C stretching vibration. The weak peak at 1663 cm⁻¹ represents the C-C stretching vibration. Whereas, the peaks located at the range 1500-1405 cm⁻¹ denote the skeletal vibration of GQDs aromatic rings, demonstrating the honeycomb lattice of graphene structure [31, 34]. C-N elongated peak at 1260 cm⁻¹ [35] and the peak at 1033 cm⁻¹ are the expression of C-O-C (epoxy group). Notably, in the GQDs/Cu₂O NCBs spectrum, the characteristic peaks of GQDs still exist, but with significantly reduced intensities. The characteristic absorption bands of Cu-O bonds in Cu₂O NCBs are also shown in the ranges 802-798 cm⁻¹ and 617-630 cm⁻¹ [36, 37]. There is also no CuO crystal formation because there is no characteristic CuO peak at positions 588, 534, and 480 cm⁻¹ [38]. This is the optically active lattice oscillation of Cu₂O, thus confirming the single pure phase nature of Cu₂O NCBs. The shift of bands in the 1700-700 cm⁻¹ region of GQDs/Cu₂O NCBs compared with the original GQDs is also due to the influence of the absorption peak of Cu-O bonds in this region [30]. Cu₂O crystals have a linear arrangement with two bonded oxygen atoms while the planar geometry of CuO crystals has four bound oxygen atoms. Therefore, the Cu(I)-O bond of Cu₂O is stronger than the Cu(II)-O bond in CuO, causing the Cu₂O peak to appear at a higher energy level. Furthermore, Cu(I) has a symmetric d¹⁰ electronic arrangement giving an equivalent Cu-O bond while CuO does not [38]. In addition, the Cu₂O peak expansion at about 630 cm⁻¹ belongs to the presence of mixed phases of the prepared sample. From that, it can be concluded that the synthesized Cu₂O NCBs have high purity. These results indicate that GQDs have been successfully combined with Cu₂O NCBs to form GQDs/Cu₂O NCBs nanocomposites.

Regarding the XRD patterns, **Fig. 3** illustrates that the synthesized GQDs possess amorphous structure, similar to the previous study [31]. The absorption intensity of the GQDs characteristic diffraction peak at an angle of $2\theta = 28^\circ$ corresponds to their (002) face. This proves that GQDs were successfully formed when using wheat flour and ascorbic acid to create graphene-structured materials through the hydrothermal method. Additionally, the XRD analysis of GQDs/Cu₂O NCBs composites demonstrate the characteristic diffraction peaks at angles of $2\theta = 29.6^\circ, 36.4^\circ, 42.3^\circ, 61.3^\circ, 73.5^\circ,$ and 77.4° , corresponding to the Cu₂O NCBs lattice planes (110), (111), (200), (220), (311), and (222), respectively [39]. These diffraction peaks completely coincide with the Cu₂O NCBs structure (JCPDS Card No. 05-0667) [13]. Thus, the peaks were assigned to the

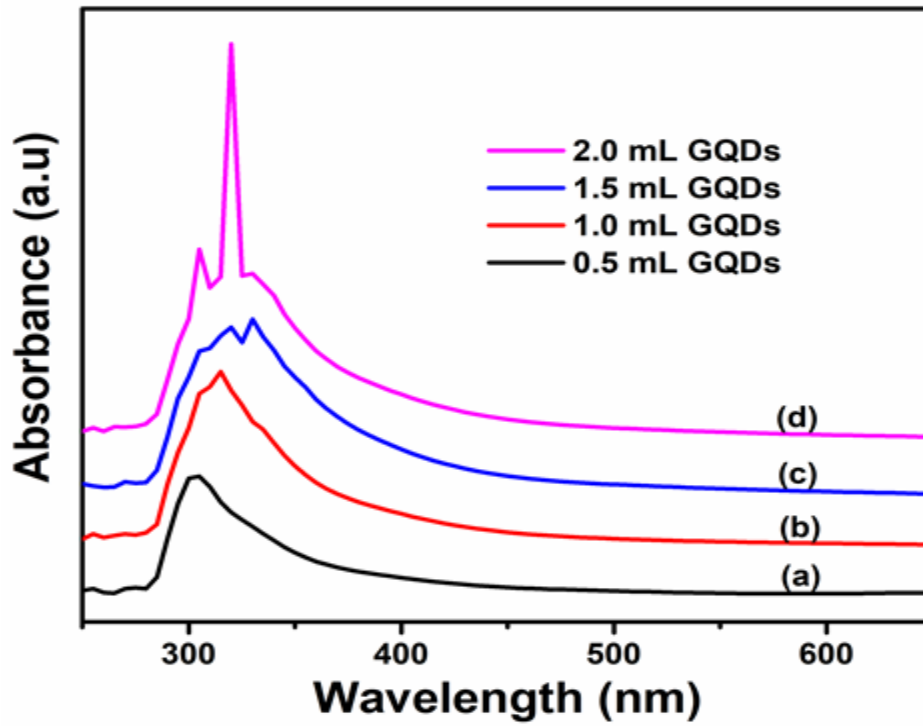


Fig. 1 UV-Vis spectra of GQDs/Cu₂O NCBs composites formulated with various GQDs solution volume of (a) 0.5 mL; (b) 1 mL; (c) 1.5 mL; and (d) 2 mL

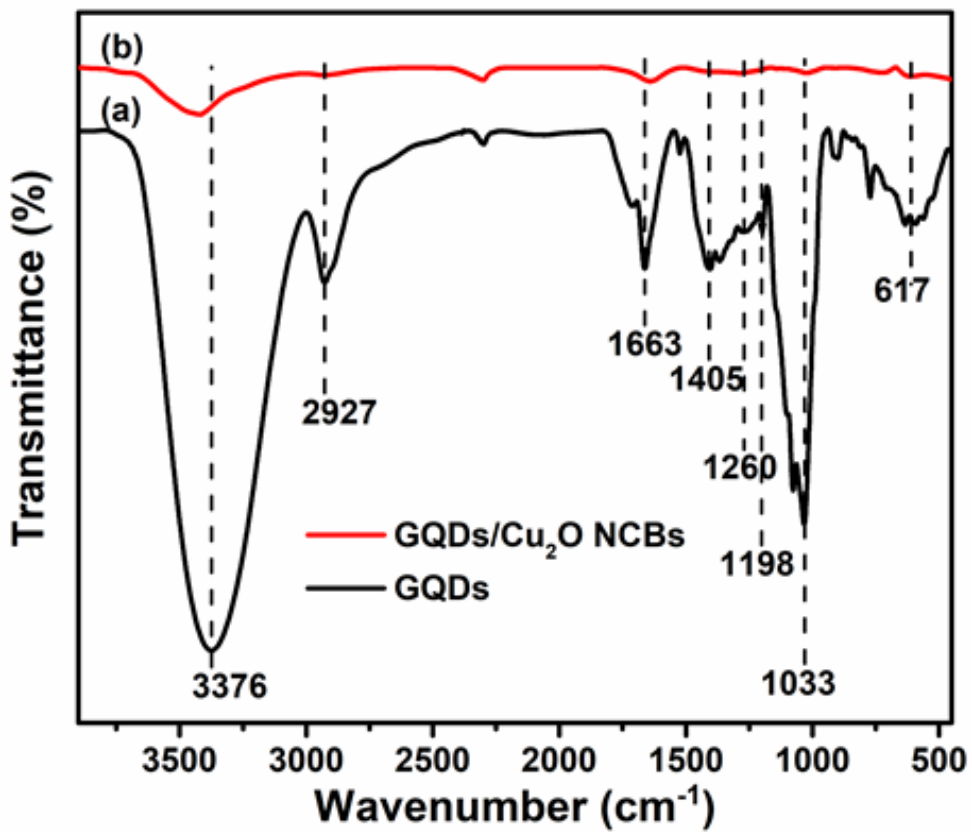


Fig. 2 Fourier transform infrared (FTIR) spectra of (a) GQDs and (b) GQDs/Cu₂O NCBs composites

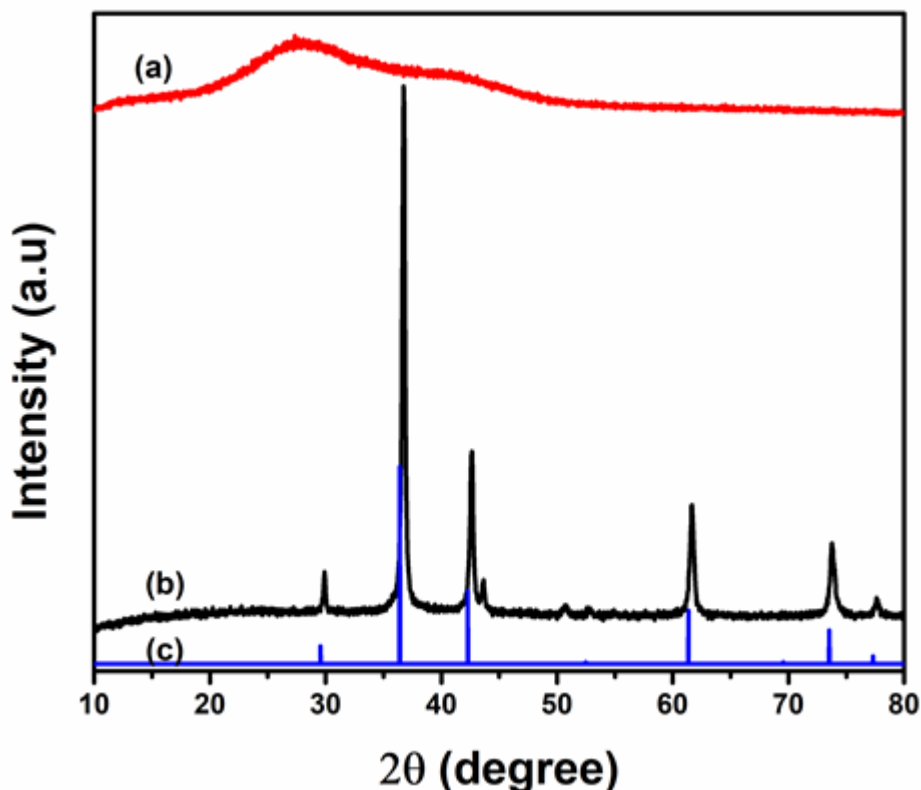


Fig. 3 X-ray diffraction (XRD) patterns of (a) GQDs and (b) GQDs/Cu₂O NCBs composites with (c) JCPDS 05-0667 data for bare Cu₂O

corresponding hkl planes. Besides, no other diffraction peaks arising from impurities such as Cu, CuO or Cu(OH)₂ were detected, thus confirming the formation of pure Cu₂O nanoparticles [40]. Conclusively, the XRD confirmed that GQDs have been successfully associated with Cu₂O NCBs to form GQDs/Cu₂O NCBs composites, which is consistent with the FTIR analyses.

The morphology of GQDs and GQDs/Cu₂O NCBs are illustrated in **Fig. 4**, TEM micrographs, which demonstrated another obvious morphological evidence for targeted GQDs/Cu₂O NCBs nanocomposites formation. For this, the GQDs were of spherical shape with an average particle size of ~3-8 nm and uniform size distribution (**Fig. 4a**). On the other hand, the Cu₂O NCBs had a cubic shape with an average particle size of ~70-80 nm, and the Cu₂O NCBs are clearly decorated with GQDs randomly distributed around (**Fig. 4b**). Furthermore, the GQDs particles did not show mutual agglomeration and agglomeration on the Cu₂O NCBs surface. It inferred that such a combination did not cause agglomeration of Cu₂O nanoparticles but also improved the surface area of the material. The reason may be related to the surface characteristics of GQDs having mainly hydroxyl, epoxy, carboxyl, and carbonyl groups. These groups exert different forces on Cu²⁺. Furthermore, the combining points with weak actions are washed away during the preparation process [41].

This result, again, was consistent with the XRD and FTIR data, indicating the successful fabrication of GQDs/Cu₂O NCBs composites.

To determine the GQDs/Cu₂O NCBs composites elemental compositions, EDX spectroscopy was employed (**Fig. 5**). The results indicate that the composites major elements include C (41.53%), O (47.03%), N (0.24%), and Cu (11.20%). The sample largest elemental content was oxygen, which mainly come from GQDs and Cu₂O, whereas the C content was from GQDs, and Cu originated from Cu₂O. Therefore, it can be confirmed that GQDs have been successfully combined with Cu₂O NCBs to form GQDs/Cu₂O NCBs nanocomposites.

3.3. Photocatalytic ability investigations of GQDs/Cu₂O NCBs composites on MB degradation

The association of GQDs on the Cu₂O NCBs surfaces allows the receipt of electrons from the excited Cu₂O, and maintains the charge stability, thereby hindering the recombination of electron and hole pairs, consequently improving the catalytic activity of the material. Moreover, the p-p interactions between the conjugate structure of GQDs and the benzene ring of MB favor the enrichment of MB on the surface of GQDs/Cu₂O NCBs composites. Thus, the photocatalytic activity of the composites on MB degradation could be theoretically

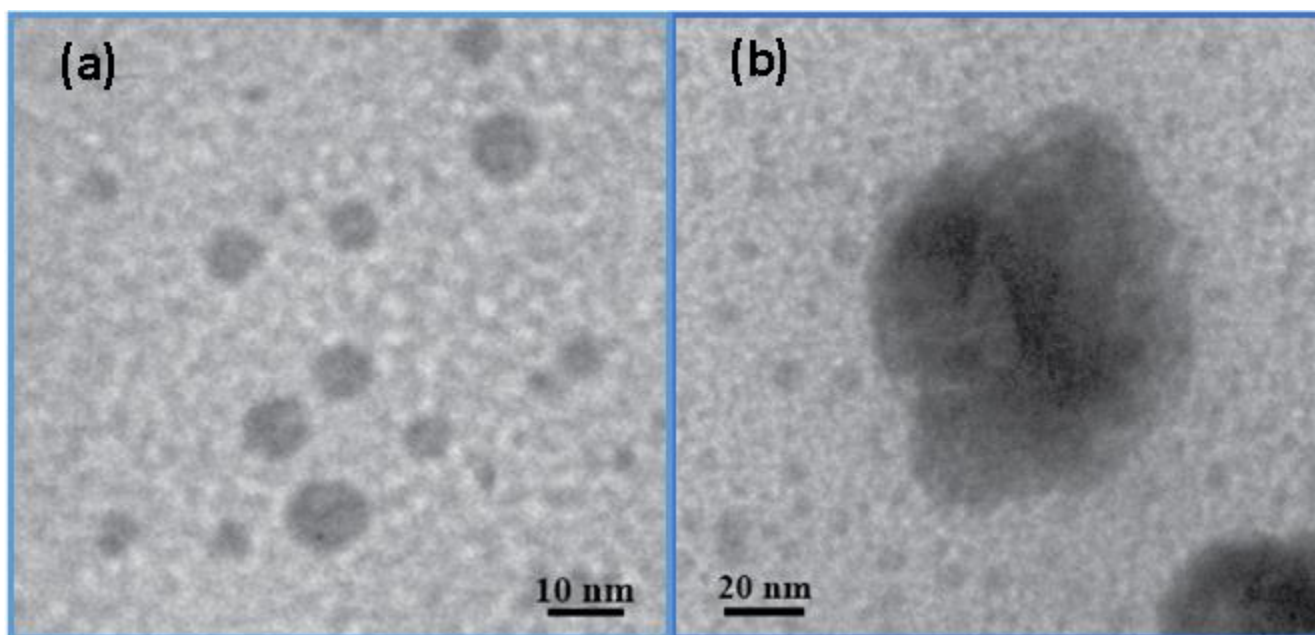


Fig. 4 TEM images of (a) GQDs and (b) GQDs/Cu₂O NCBs composites

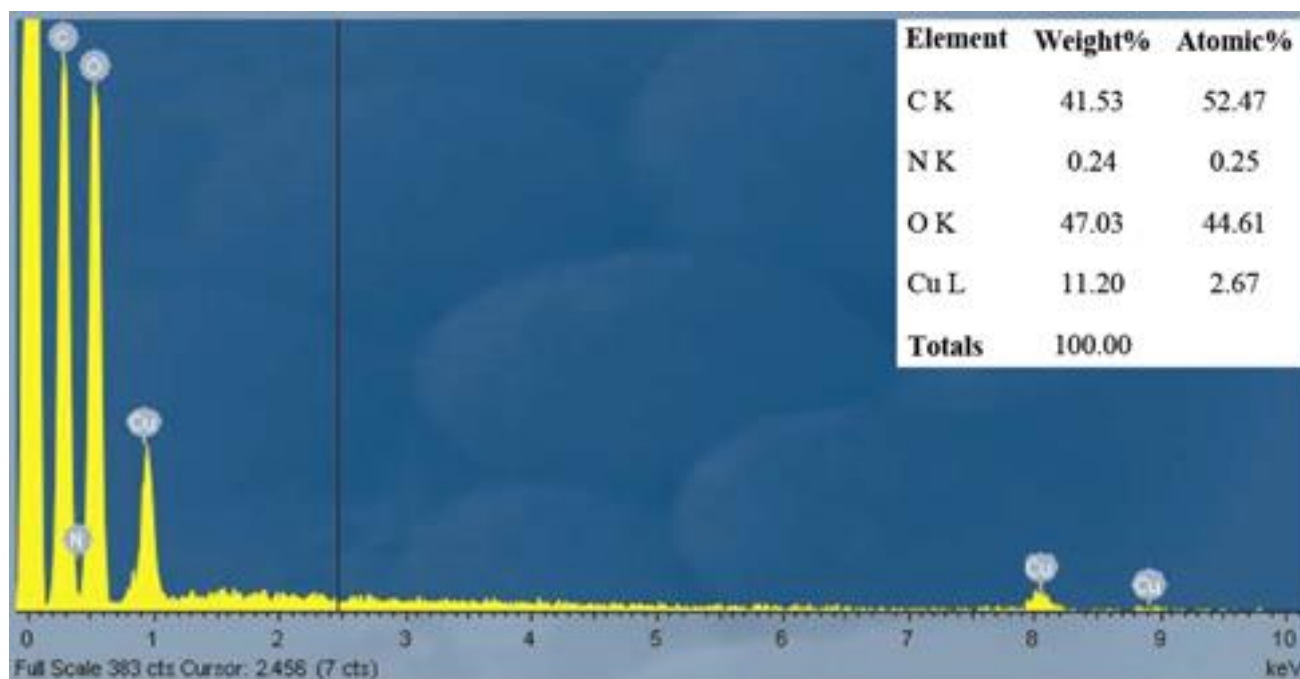


Fig. 5 Energy dispersive X-ray (EDX) spectra of GQDs/Cu₂O NCBs composites

increased. Herein, we investigated the effects of GQDs/Cu₂O NCBs amount/volume and the absorption time on the MB degradation.

Expectedly, **Fig. 6a** shows that the addition of GQDs/Cu₂O NCBs significantly reduced the absorption intensity of MB molecules on the UV-Vis spectra. Research shows that, one unit volume reasonably increases the probability of collision between organics and oxidants, resulting in increased decolorization efficiency. It can be seen that increasing the amount of catalyst increases the number of both dye molecules

adsorbed and photons absorbed; thereby increasing the number of hydroxyl radicals, and enhancing the degradation of MB [42, 43]. This reduction was in proportion to the increase of the composites volume from 0 to 750 μ L and achieved the highest treatment efficiency at 98.03% for reducing of MB with respective amount of GQDs/Cu₂O NCBs composites being 750 μ L – see **Fig. 6b**. Interestingly, when the composites volume increased from 750 to 1000 μ L, the MB degradation rate decreased (with the gradual decreasing of treatment efficiency respective obtained being 98.03% and 97.15% – see **Fig. 6b**. This could be

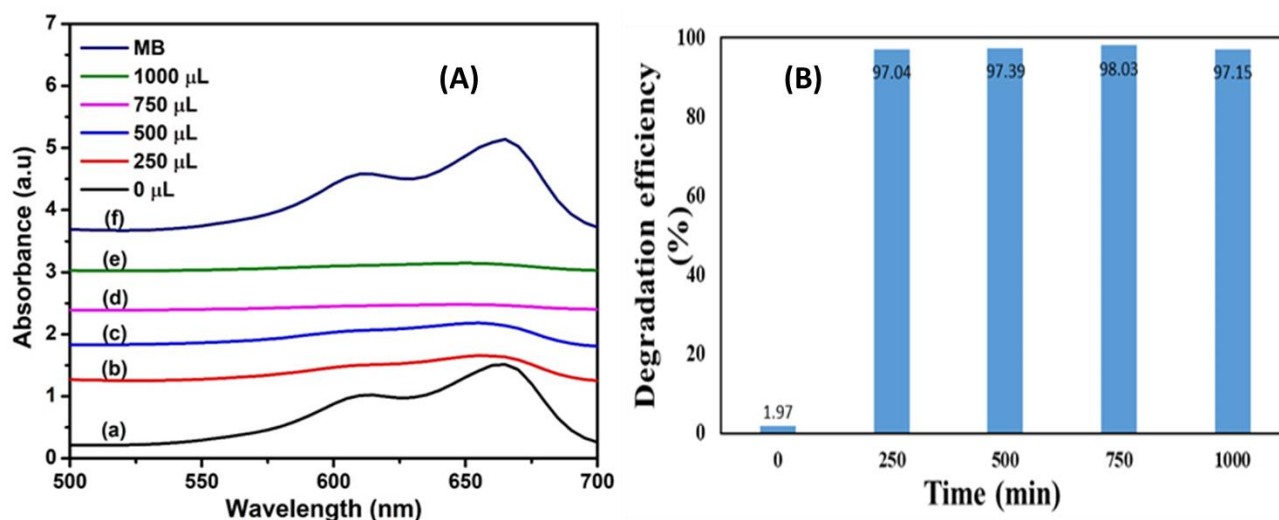


Fig. 6 A) UV-Vis spectra of methylene blue (MB) solution with different GQDs/Cu₂O NCBs volumes of (a) 0 μ L, (b) 250 μ L, (c) 500 μ L, (d) 750 μ L, (e) 1000 μ L, and (f) MB. **B**) The percent degradation of MB corresponds to different volumes of GQDs/Cu₂O NCBs at pH = 7 after 30 min of reaction

explained by the overlapping amongst the catalyst materials when too many particles are presented simultaneously in the solution, thus reducing their ability to contact H₂O₂ and to be excited by light. Consequently, less \cdot OH was generated and the MB degradation rate decreased.

The optimal GQDs/Cu₂O NCBs volume of 750 μ L was then employed in the absorption time-variation experiments (Fig. 7). The UV-vis spectrum showed no new peaks in the UV region, confirming that many MB molecules were mineralized during this decomposition. Previously published studies on monomers and oligomers (dimer and trimer) of MB in aqueous solution had UV-Vis absorption maxima at 668 and 624 nm [44]. This study shows good agreement with these observations. MB's 664 nm wavelength has a strongly reduced absorption strength suggesting that the MB monomer may have broken down rapidly while its dimer or trimer may be more difficult to break and will degrade for a longer time. Because MB dimer has higher molar absorptivity than its monomer, it has higher stability due to higher resonance [45]. The shoulder at 610 nm belongs to MB's dimer. During this decomposition, the main MB absorption peak at 664 nm was rapidly decreased and was followed by a decrease of the minor peak at 610 nm. This confirms that the parent MB molecule has degraded to some new intermediates that are structurally close to the parent compound with slight structural differences, such as those with a lesser methyl groups [44]. Besides, the MB degradation efficiency of GQDs/Cu₂O NCBs composites catalyst increased proportionally to the treatment time (with increasing of treatment efficiency

from 22.82% to 98.43% – see Fig. 7b and achieved the high treatment efficiency >98% when treatment time gradually increasing from 30 min to 40 min – see in Fig. 7b. Thus, the absorption process was time dependent.

Chemical reactions include breaking old bonds and forming new ones. The decomposition mechanism of methylene blue can be described as follows. During the dissolution of the methylene blue molecule, Cl⁻ is first ionized and exists in the dissociated state. N – CH₃, joined to 7C or 12C, has the lowest bond dissociation energy (BDE) value in the methylene blue molecular structure. During radical bombardment, the N – CH₃ bond is first broken and –CH₃ is oxidized to HCHO or HCOOH. C – S and C – N are the most active parts of the remaining structure of the methylene blue molecule. During bombardment OH \cdot and O₃, these two bonds are more easily broken. Simultaneously, phenyl thiophene may also be formed. In the latter stage, a variety of radicals in the methylene blue solution are generated. These organic molecular structures are oxidized until they are finally converted to inorganic ions, such as CO₂, H₂O, Cl⁻, SO₄²⁻ and NO₃⁻ [46, 47].

4. Conclusions

The present study reported a novel composites material fabricated from graphene quantum dots (GQDs) and cuprous oxide nanocubes (Cu₂O NCBs), namely GQDs/Cu₂O NCBs, to enhance the photocatalytic activity of the cuprous oxide nanocubes, tested with MB degradation as an application. The GQDs/Cu₂O NCBs were successfully formulated, confirmed by the UV-Vis, FTIR, XRD, EDX, and TEM analyses, the results show that the formed GQDs have been successfully

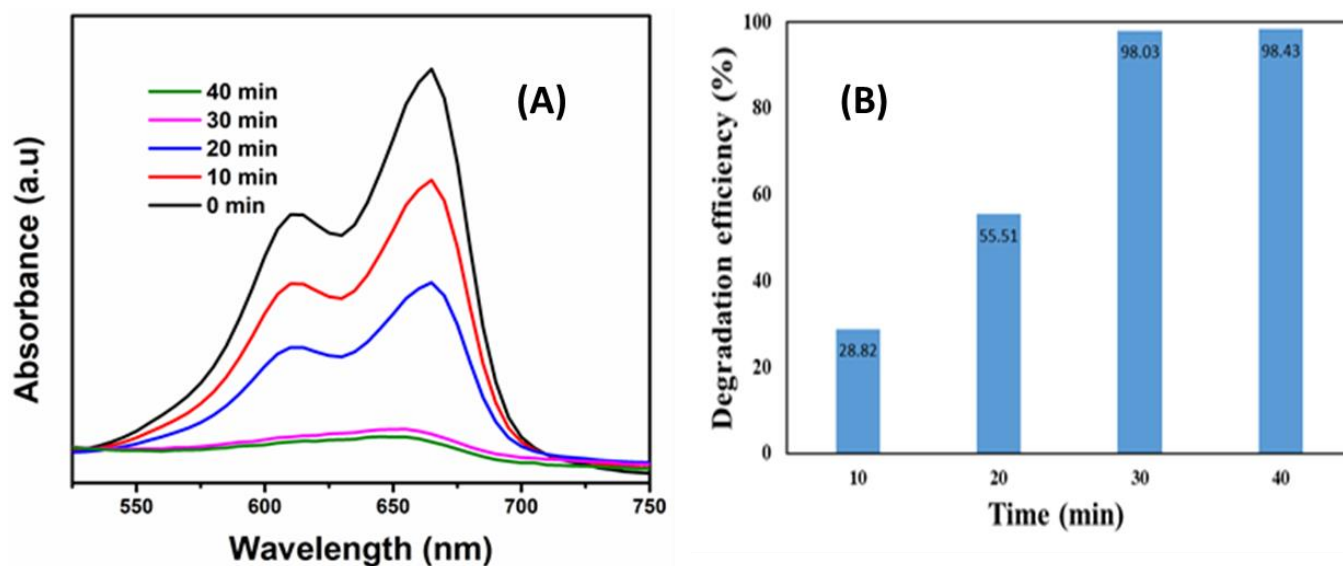


Fig. 7 A) UV-Vis spectra of methylene blue (MB) solution and GQDs/Cu₂O NCBs with different absorption time of (a) 0 min, (b) 10 min, (c) 20 min, (d) 30 min, and (e) 40 min at pH = 7. **Fig. 7. B)** Percent degradation versus different reaction time for MB reduction with 750 µL GQDs/Cu₂O NCBs at pH = 7

combined with high purity Cu₂O NCBs. Regarding the photocatalytic activity, the GQDs/Cu₂O NCBs, with a little amount of 750 µL, could effectively degrade >98% of MB within 30 min. Conclusively, the novel GQDs/Cu₂O NCBs composites possessed potential catalytic activity and could be utilized as photocatalysts in the treatment of organic pollutants and biological waste such as dyes, antibiotics, pesticides, and the like.

Acknowledgements

This research is funded by Vietnam Ministry of Education and Training under grant number B2022-TCT-08.

References

- [1] Y. Wen, G. Schoups, N. Van De Giesen, Organic pollution of rivers: Combined threats of urbanization, livestock farming and global climate change, *Sci. Rep.* 7(1) (2017) 1-9.
- [2] A. Nezamzadeh-Ejehieh, E. Shahriari, Photocatalytic decolorization of methyl green using Fe (II)-o-phenanthroline as supported onto zeolite Y, *J. Indust. Eng. Chem.* 20(5) (2014) 2719-2726.
- [3] H. Alkallas, A. Ben Gouider Trabelsi, R. Nasser, S. Fernandez, J.M. Song, H. Elhouichet, Promising Cr-Doped ZnO Nanorods for Photocatalytic Degradation Facing Pollution, *Appl. Sci.* 12(1) (2022) 34.
- [4] A. Mallick, P.D. Patil, M.S. Tiwari, P. Kane, D. Khonde, Green and sustainable methods for dye degradation employing photocatalytic materials, *Photocatalytic Degradation of Dyes*, Elsevier2021, pp. 345-376.
- [5] H. Derikvandi, A. Nezamzadeh-Ejehieh, A comprehensive study on enhancement and optimization of photocatalytic

activity of ZnS and SnS₂: Response Surface Methodology (RSM), nn heterojunction, supporting and nanoparticles study, *J. Photochem. Photobio. A: Chem.* 348 (2017) 68-78.

[6] B. Divband, A. Jodaei, M. Khatamian, Enhancement of photocatalytic degradation of 4-nitrophenol by integrating Ag nanoparticles with ZnO/HZSM-5 nanocomposite, *Iran. J. Catal.* 9(1) (2019) 63-70.

[7] P. Falcaro, R. Ricco, A. Yazdi, I. Imaz, S. Furukawa, D. Maspoeh, R. Ameloot, J.D. Evans, C.J. Doonan, Application of metal and metal oxide nanoparticles@MOFs, *Coordin. Chem. Rev.* 307 (2016) 237-254.

[8] Q. Wang, Y. Zhu, J. Xue, X. Zhao, Z. Guo, C. Wang, General synthesis of porous mixed metal oxide hollow spheres with enhanced supercapacitive properties, *ACS Appl. Mater. Inter.* 8(27) (2016) 17226-17232.

[9] M.-G. Kim, M.G. Kanatzidis, A. Facchetti, T.J. Marks, Low-temperature fabrication of high-performance metal oxide thin-film electronics via combustion processing, *Nature Mater.* 10(5) (2011) 382-388.

[10] R. Chen, J. Lu, Z. Wang, Q. Zhou, M. Zheng, Microwave synthesis of Cu/Cu₂O/SnO₂ composite with improved photocatalytic ability using SnCl₄ as a protector, *J. Mater. Sci.* 53(13) (2018) 9557-9566.

[11] B. Peng, S. Zhang, S. Yang, H. Wang, H. Yu, S. Zhang, F. Peng, Synthesis and characterization of g-C₃N₄/Cu₂O composite catalyst with enhanced photocatalytic activity under visible light irradiation, *Mater. Res. Bulletin.* 56 (2014) 19-24.

[12] T. Aditya, J. Jana, N.K. Singh, A. Pal, T. Pal, Remarkable facet selective reduction of 4-nitrophenol by morphologically tailored (111) faceted Cu₂O nanocatalyst, *ACS Omega* 2(5) (2017) 1968-1984.

- [13] A.K. Sasmal, S. Dutta, T. Pal, A ternary Cu₂O–Cu–CuO nanocomposite: a catalyst with intriguing activity, *Dalton Trans.* 45(7) (2016) 3139-3150.
- [14] H. Derikvandi, M. Vosough, A. Nezamzadeh-Ejchieh, A comprehensive study on the enhanced photocatalytic activity of a double-shell mesoporous plasmonic Cu@Cu₂O/SiO₂ as a visible-light driven nanophotocatalyst, *Environ. Sci. Poll. Res.* 27 (2020) 27582-27597.
- [15] X. Zhao, Y. Li, Y. Guo, Y. Chen, Z. Su, P. Zhang, Coral-like MoS₂/Cu₂O porous nanohybrid with dual-electrocatalyst performances, *Adv. Mater. Inter.* 3(23) (2016) 1600658.
- [16] W. Sang, G. Zhang, H. Lan, X. An, H. Liu, The effect of different exposed facets on the photoelectrocatalytic degradation of o-chlorophenol using p-type Cu₂O crystals, *Electrochim. Acta* 231 (2017) 429-436.
- [17] M. Wang, L. Sun, Z. Lin, J. Cai, K. Xie, C. Lin, p–n Heterojunction photoelectrodes composed of Cu₂O-loaded TiO₂ nanotube arrays with enhanced photoelectrochemical and photoelectrocatalytic activities, *Energ. Environ. Sci.* 6(4) (2013) 1211-1220.
- [18] Y.H. Chang, M.Y. Chiang, J.H. Chang, H.N. Lin, Enhanced visible light photocatalysis of cuprous oxide nanoparticle modified zinc oxide nanowires, *Mater. Lett.* 138 (2015) 85-88.
- [19] W.J. Ong, L.L. Tan, Y.H. Ng, S.T. Yong, S.P. Chai, Graphitic carbon nitride (g-C₃N₄)-based photocatalysts for artificial photosynthesis and environmental remediation: are we a step closer to achieving sustainability?, *Chem. Rev.* 116(12) (2016) 7159-7329.
- [20] C. Ye, J.X. Li, Z.J. Li, X.B. Li, X.B. Fan, L.P. Zhang, B. Chen, C.H. Tung, L.Z. Wu, Enhanced driving force and charge separation efficiency of protonated g-C₃N₄ for photocatalytic O₂ evolution, *ACS Catal.* 5(11) (2015) 6973-6979.
- [21] F. Bonaccorso, Z. Sun, T. Hasan, A. Ferrari, Graphene photonics and optoelectronics, *Nature Photon.* 4(9) (2010) 611-622.
- [22] Z. Wu, Y. Huang, L. Xiao, D. Lin, Y. Yang, H. Wang, Y. Yang, D. Wu, H. Chen, Q. Zhang, Physical properties and structural characterization of starch/polyvinyl alcohol/graphene oxide composite films, *Inter. J. Biolog. Macro.* 123 (2019) 569-575.
- [23] L. Li, G. Wu, G. Yang, J. Peng, J. Zhao, J.J. Zhu, Focusing on luminescent graphene quantum dots: current status and future perspectives, *Nanoscale* 5(10) (2013) 4015-4039.
- [24] M.H. Facure, R. Schneider, L.A. Mercante, D.S. Correa, A review on graphene quantum dots and their nanocomposites: from laboratory synthesis towards agricultural and environmental applications, *Environ. Sci.: Nano* 7(12) (2020) 3710-3734.
- [25] S. Kumar, A. Dhiman, P. Sudhagar, V. Krishnan, ZnO-graphene quantum dots heterojunctions for natural sunlight-driven photocatalytic environmental remediation, *Appl. Surf. Sci.* 447 (2018) 802-815.
- [26] A. Kalluri, D. Debnath, B. Dharmadhikari, P. Patra, Graphene quantum dots: synthesis and applications, *Methods in enzymology* 609 (2018) 335-354.
- [27] C. Zhao, X. Song, Y. Liu, Y. Fu, L. Ye, N. Wang, F. Wang, L. Li, M. Mohammadniaei, M. Zhang, Synthesis of graphene quantum dots and their applications in drug delivery, *J. Nanobiotech.* 18(1) (2020) 1-32.
- [28] L. Fang, Q. Xu, X. Zheng, W. Zhang, J. Zheng, M. Wu, W. Wu, Soy flour-derived carbon dots: facile preparation, fluorescence enhancement, and sensitive Fe³⁺ detection, *J. Nanopart. Res.* 18(8) (2016) 1-13.
- [29] M. Batool, D. Hussain, A. Akrem, M. Najam-ul-Haq, S. Saeed, S.M. Zaka, M.S. Nawaz, F. Buck, Q. Saeed, Graphene quantum dots as cysteine protease nanocarriers against stored grain insect pests, *Sci. Rep.* 10(1) (2020) 1-11.
- [30] Asar Ahmed, Namdeo S. Gajbhiye, Amish G. Joshi, Low cost, surfactant-less, one pot synthesis of Cu₂O nano-octahedra at room temperature, *J. Solid State Chem.* 184 (2011) 2209–2214.
- [31] W. Chen, D. Li, L. Tian, W. Xiang, T. Wang, W. Hu, Y. Hu, S. Chen, J. Chen, Z. Dai, Synthesis of graphene quantum dots from natural polymer starch for cell imaging, *Green Chem.* 20(19) (2018) 4438-4442.
- [32] C.P. Deming, R. Mercado, V. Gadiraju, S.W. Sweeney, M. Khan, S. Chen, Graphene quantum dots-supported palladium nanoparticles for efficient electrocatalytic reduction of oxygen in alkaline media, *ACS Sustain. Chem. Eng.* 3(12) (2015) 3315-3323.
- [33] D. Sun, R. Ban, P.H. Zhang, G.H. Wu, J.R. Zhang, J.J. Zhu, Hair fiber as a precursor for synthesizing of sulfur-and nitrogen-co-doped carbon dots with tunable luminescence properties, *Carbon* 64 (2013) 424-434.
- [34] J. Chen, Z. Long, S. Wang, Y. Meng, G. Zhang, S. Nie, Biodegradable blends of graphene quantum dots and thermoplastic starch with solid-state photoluminescent and conductive properties, *Inter. J. Biological Macro.* 139 (2019) 367-376.
- [35] M. Vandana, S. Ashokkumar, H. Vijeth, L. Yesappa, H. Devendrappa, Synthesis and characterization of polypyrrole-graphene quantum dots nanocomposites for supercapacitor application, *AIP Conference Proceedings*, AIP Publishing LLC, 2019, p. 030535.
- [36] W.C.J. Ho, Q. Tay, H. Qi, Z. Huang, J. Li, Z. Chen, Photocatalytic and adsorption performances of faceted cuprous oxide (Cu₂O) particles for the removal of methyl orange (MO) from aqueous media, *Molecules* 22(4) (2017) 677.
- [37] A. Norouzi, A. Nezamzadeh-Ejchieh, R. Fazaeli, A Copper (I) oxide-zinc oxide nano-catalyst hybrid: Brief characterization and study of the kinetic of its photodegradation and photomineralization activities toward

methylene blue, *Mater. Sci. Semiconduct. Process.* 122 (2021) 105495.

[38] M. Kouti, L. Matouri, Fabrication of nanosized cuprous oxide using fehling's solution, *Scientia Iranica* 17(1) (2010) 73-78.

[39] Y. Guo, M. Dai, Z. Zhu, Y. Chen, H. He, T. Qin, Chitosan modified Cu₂O nanoparticles with high catalytic activity for p-nitrophenol reduction, *Appl. Surf. Sci.* 480 (2019) 601-610.

[40] Chunhua Cao, Ling Xiao, Preparation and visible-light photocatalytic activity of Cu₂O/PVA/Chitosan composite films, *Adv. Mater. Res.* 1015 (2014) 623-626.

[41] A. Wang, X. Li, Y. Zhao, W. Wu, J. Chen, H. Meng, Preparation and characterizations of Cu₂O/reduced graphene oxide nanocomposites with high photo-catalytic performances, *Powder Tech.* 261 (2014) 42-48.

[42] M. Karimi-Shamsabadi, A. Nezamzadeh-Ejehieh, Comparative study on the increased photoactivity of coupled and supported manganese-silver oxides onto a natural zeolite nano-particles, *J. Mol. Catal. A: Chem.* 418 (2016) 103-114.

[43] M. Kasiri, H. Aleboyeh, A. Aleboyeh, Degradation of Acid Blue 74 using Fe-ZSM5 zeolite as a heterogeneous photo-Fenton catalyst, *Appl. Catal. B: Environ.* 84(1-2) (2008) 9-15.

[44] S. Senobari, A. Nezamzadeh-Ejehieh, A comprehensive study on the photocatalytic activity of coupled copper oxide-cadmium sulfide nanoparticles, *Spectrochimica Acta Part A: Molecular Biomolecular Spectroscopy* 196 (2018) 334-343.

[45] M.A. Rauf, M.A. Meetani, A. Khaleel, A. Ahmed, Photocatalytic degradation of methylene blue using a mixed catalyst and product analysis by LC/MS, *Chem. Eng. J.* 157(2-3) (2010) 373-378.

[46] F. Huang, L. Chen, H. Wang, Z. Yan, Analysis of the degradation mechanism of methylene blue by atmospheric pressure dielectric barrier discharge plasma, *Chem. Eng. J.* 162(1) (2010) 250-256.

[47] A. Nezamzadeh-Ejehieh, S. Hushmandrad, Solar photodecolorization of methylene blue by CuO/X zeolite as a heterogeneous catalyst, *Appl. Catal. A: General* 388(1-2) (2010) 149-159.